



International Journal for Innovative Engineering and Management Research

A Peer Reviewed Open Access International Journal

www.ijiemr.org

COPY RIGHT



ELSEVIER
SSRN

2019IJIEMR. Personal use of this material is permitted. Permission from IJIEMR must be obtained for all other uses, in any current or future media, including reprinting/republishing this material for advertising or promotional purposes, creating new collective works, for resale or redistribution to servers or lists, or reuse of any copyrighted component of this work in other works. No Reprint should be done to this paper, all copy right is authenticated to Paper Authors

IJIEMR Transactions, online available on 4th Sept 2019. Link

[:http://www.ijiemr.org/downloads.php?vol=Volume-08&issue=ISSUE-09](http://www.ijiemr.org/downloads.php?vol=Volume-08&issue=ISSUE-09)

Title **MODIFIED Z-SOURCE UNIFIED EVDC CHARGER DESIGN**

Volume 08, Issue 09, Pages: 302–311.

Paper Authors

K SAI PRIYA, M DURGA PRASAD, K TAGORE

Anu Bose Institute of Technology K.S.P Road, New paloncha, Bhadradi Kothagudem, Telangana, India



USE THIS BARCODE TO ACCESS YOUR ONLINE PAPER

To Secure Your Paper As Per **UGC Guidelines** We Are Providing A Electronic Bar Code

MODIFIED Z-SOURCE UNIFIED EVDC CHARGER DESIGN

K SAI PRIYA¹, M DURGA PRASAD², K TAGORE³

^{1,2,3}UG Students, Dept. of Electrical and Electronics Engineering, Anu Bose Institute of Technology, KSPRoad, NewPaloncha, Bhadradi Kothagudem, Telangana, India.

priyaammulu789@gmail.com¹, durgacool635@gmail.com², tagorekodem143@gmail.com³

Abstract:- Sun based Energy has been the most well known wellsprings of sustainable power source for private and semi business applications. Changes of sun oriented vitality gathered because of air conditions can be relieved through vitality stockpiling frameworks. Sunlight based vitality can likewise be utilized to charge electric vehicle batteries to diminish the reliance on the lattice. One of the prerequisites for a converter for such applications is to have a diminished no. of change arranges & give confinement. Z-source inverter (ZSI) topology can evacuate different stages and accomplish voltage lift and DC-AC control transformation in a solitary stage. The utilization of a split parts additionally displays a chance to incorporate vitality stockpiling frameworks (ESS) into them. This article presents displaying, plan and activity of a changed Z-source inverter (MZSI) incorporated with a split essential disconnected battery charger for DC charging of electric vehicles (EV) batteries. Reproduction and test results have been introduced for the evidence of idea of the activity of the proposed converter.

Index Terms:- Z-source-inverters; Active filter; Energy Storage; photovoltaic (PV) power generation; quasi-Zsource inverter (qZSI); Single-Phase Systems; transportation electrification; Solar energy; distributed power generation, inverter.

I. INTRODUCTION

CHARGING of electric vehicles at present intensely includes utilization of AC framework. The different strategies for charging only use AC lattice, for example, remote charging or module charging can at present reason contamination independent of how profoundly proficient the topology is. The measure of petroleum derivatives that are expended to produce the vitality to charge an electric vehicle gives a more clear image of the carbon impression that is deserted while charging an electric vehicle. To accomplish lower carbon impressions, one of the ways is to incorporate sustainable power sources into a charging framework to diminish the reliance on the AC lattice. A noteworthy necessity for planning an EV battery charger is the

utilization of disconnection transformers in the converter topologies, give galvanic seclusion at the client end from the remainder of the high voltage (HV) framework as a security measure [1]. The galvanic seclusion can be given either on the AC matrix side or on the charger side. The size of the confinement transformer on the lattice side is typically a lot bigger than the one on the charger side [2]. Because of the improvement in semiconductor innovation, high recurrence exchanging encourages the utilization of smaller size transformers for galvanic disconnection. Photovoltaic matrix interconnected frameworks have been utilized in the past for business charging foundation [3]. These frameworks decrease the reliance of the

charging foundation on the AC network. The utilization of sunlight based and lattice interconnected framework is an appealing answer for private charging frameworks for EVs. For frameworks upto 10 kW, single stage inverters can be utilized for private applications [4][5]. For interconnection of the private sun based PV to the lattice, different disconnected and non segregated topologies are accessible with various stages [4][6]. Private photovoltaic frameworks for EV charging require highlights, for example, seclusion and voltage support capability to coordinate the sun powered PV cluster voltage to the lattice voltage prerequisites. The ZSI topology was first presented in [7]. It has a capacity to buck or support and alter the information DC voltage in a solitary stage. It has increased enormous enthusiasm for photovoltaic-network associated applications. The ZSI

topology utilizes two capacitors and two inductors to support the information DC voltage to coordinate the inverter side AC yield voltage prerequisites. The activity of a ZSI is vigorously reliant on the uninvolvement parts. It introduces a chance to incorporate vitality stockpiling units into such a framework. In this paper a proof of idea of a solitary stage MZSI based sun oriented matrix associated charger has been displayed as an application towards a string inverter setup. In area II, the fundamental activity standard for a ZSI have been talked about alongside the part plan. Segment III, examines the measuring of parts, demonstrating and control of the converter. Segment IV, displays the reproduction results for the activity of a 3.3 kW proposed inverter charger and results from a test arrangement worked as a proof of idea. Segment V, displays the end.

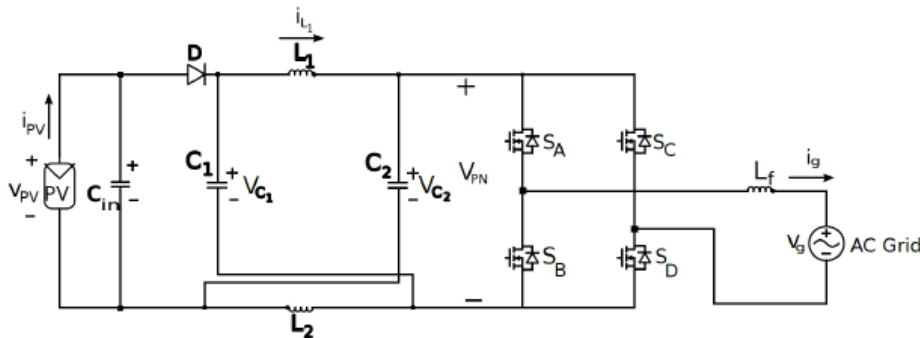


Fig. 1. Schematic of a Photovoltaic/AC grid inter-connected Z-source Inverter(ZSI)

II. TRADITIONAL ZSI

The ZSI topology, appeared in Fig.1, uses two methods of activity: the shoot through state and the non-shoot through state [7]. For symmetrical tasks,

$$i_L = i_{L1} = i_{L2} \quad (1)$$

$$V_C = V_{C1} = V_{C2} \quad (2)$$

From Fig.1, in the shoot through express, every one of the four switches, S1, S3, S2 and S4, are leading simultaneously. The

term of this shoot through state is depicted by the obligation cycle D_0 and the exchanging recurrence FSW.

The shoot through state can be executed by a changed PWM method exhibited in [7]. Accordingly, the two capacitor voltages are communicated as [7]:

$$V_C = \frac{1 - D_0}{1 - 2D_0} v_{pv} \quad (3)$$

Subsequently, keeping up a higher pinnacle voltage at the contribution of the DC interface, V_{PN} . The pinnacle DC connect voltage, V_{PN}^{\wedge} , is given by[7]:

$$V_{PN}^{\wedge} = \frac{1}{1 - 2D_0} v_{pv} \quad (4)$$

The powerbalance condition between the DC and AC side of the ZSI is communicated as [7],

$$(1 - D_0)V_{PN}^{\wedge}I_{PN} = i_{grms}v_{grms} \quad (5)$$

Where I_{PN} and V_{PN}^{\wedge} are the pinnacle DC interface current and voltage. The pinnacle AC voltage of the ZSI is [7]:

$$V_g = MV_{PN}^{\wedge} \quad (6)$$

where the M is the modulation index, grid voltage, $v_g = V_g \sin \omega t$ and the grid current $i_g = I_g \sin(\omega t + \phi)$. For $\phi = 0$ for grid connected applications. From equation (11) and (13) the RMS of the output AC voltage of the ZSI is [7]:

$$V_{grms} = \frac{Mv_{pv}}{\sqrt{2}(1 - 2D_0)} \quad (7)$$

III. COMPONENT SIZING, MODELING AND CONTROL OF PROPOSED MZSI

Fig. 2 demonstrates a changed Z source inverter has been proposed having an incorporated charger. The MOSFET SR permits bidirectional activity of the MZSI when required. The diode DPV obstructs the turn around stream of current once again into the PV. R_{in} is the interior opposition of the info capacitor C_{in} . For symmetrical activity of the MZSI, a split essential segregated DC to DC converter has been proposed for the joining of the charger side into the ZSI. The split primaries contain two half extension converter (HBC) primaries confined from a solitary full scaffold optional through a high recurrence transformer. The HBC primaries and the secondaries are worked at half obligation

cycle in open circle. The yield current of the auxiliary is associated with a vitality stockpiling unit, for example, a lithium-particle (Li-particle) battery. The vitality stockpiling unit cinches its own voltage, v_B , over the contribution of the HBC primaries, V_C , with the end goal that,

$$V_C = 2v_B \quad (8)$$

A. Maximum Shoot Through Duty Ratio, D_{0max}

Because of the vitality stockpiling unit being associated over the capacitors, the most extreme shoot through obligation proportion, D_{0max} is determined dependent on the base information voltage, v_{pvmin} and the greatest battery voltage, V_{Bmax} associated over the capacitors and is communicated as:

$$D_{0max} = \frac{2V_{Bmax} - v_{pvmin}}{4V_{Bmax} - v_{pvmin}} \quad (9)$$

SAE J1772 standard defines the standard battery voltages for DC charging between 200V-500V.

B. Inductor L_1 and L_2 design

The inductors L_1 and L_2 are estimated for high recurrence top to top current swell expected between 15-25% of the Fig. 2. Point by point Schematic of Proposed MZSI inductor current during the shoot through time interim $\frac{D_0 T}{2}$ as follow [8]:

$$L_1 = L_2 = \frac{V_{Cmax} D_{0max}}{2\Delta i_L f} \quad (10)$$

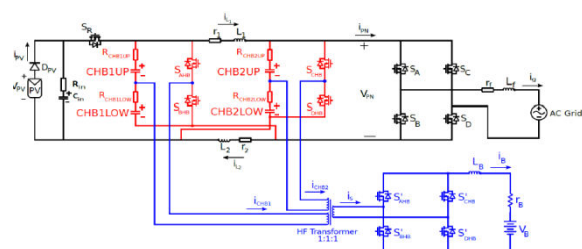


Fig. 2. Detailed Schematic of Proposed MZSI

C. Capacitor C₁ and C₂ design

The capacitors are measured to retain the second request symphonious part in the capacitor voltages as pursue [8]:

$$L_1 = L_2 = \frac{V_{Cmax} D_{0max}}{2\Delta i_L f}$$

where V_C is the normal voltage over the capacitors V_{C1} and V_{C2} and ΔV_C is the foreordained voltage swell point of confinement. ω is the second request sounds communicated in rad/s. In single stage Z source inverters, curiously large electrolytic capacitors for second request music concealment can bring about a cumbersome framework. A DC side Active Power Filter (APF) proposed in [9], can be utilized to lessen the capacitance required. It works autonomous of the activity of the MZSI. For the proposed topology, most extreme capacitor voltage rating is equivalent to at least double the pinnacle voltage of the vitality stockpiling gadget clasped crosswise over it.

D. Average Modeling of the Integrated Half-Bridge DCDC Converter Charger

At the point a vitality stockpiling unit is associated with the auxiliary side of the charger then every one of the split primaries works on the other hand and supplies a large portion of battery. Every one of the primaries of the DC-DC converter is associated over the capacitors of either legs. The voltage over the capacitors is characterized by the condition (15). The definite normal displaying of the split essential DC-DC converter is clarified in [10]. Every one of the two primaries can be spoken to utilizing a RLE circuit associated parallel to every one of the capacitor, C₁ and C₂, as appeared in the simplified proportional model of the Fig. 4.

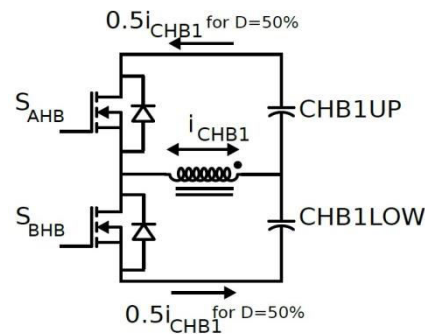


Fig. 3. Schematic of one the Primary across CHB1 operating at 50% duty cycle.

E. State Space Average Modeling of the Single Stage Inverter Charger

The nitty gritty state space normal displaying was introduced in [10]. The equal graph of the demonstrated MZSI is shown in the Fig. 4, During the non shoot-through express, the KVL condition is given by:

$$L \frac{di_L}{dt} = v_{pv} - i_L r + R_{HB} + (2\hat{i}_g + \frac{i_B}{2}) R_{HB} - V_C$$

The KCL equation is:

$$C \frac{dV_C}{dt} = i_L - \hat{i}_g - \frac{i_B}{4} \quad (13)$$

During the shoot-through express, the KVL condition is:

$$L \frac{di_L}{dt} = V_C - i_L (R_{HB} + r) - \frac{i_B}{2} R_{HB} \quad (14)$$

The KCL equation is written as:

$$C \frac{dV_C}{dt} = -i_L - \frac{i_B}{4} \quad (15)$$

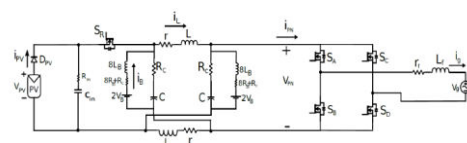


Fig. 4. Equivalent Model of the proposed Modified Z-source Inverter (MZSI) with battery

From condition (12)- (15), state space conditions for the whole framework can be composed as:

$$\begin{aligned}
 \begin{bmatrix} \dot{i}_L \\ \dot{V}_C \\ \dot{i}_B \end{bmatrix} &= \begin{bmatrix} \frac{-(r+2R_{HB})}{L} & \frac{1-2D_0}{L} & \frac{(1-2D_0)R_{HB}}{2} \\ \frac{1-2D_0}{C} & 0 & -\frac{1}{4C} \\ \frac{1-2D_0}{L_B}R_{HB} & \frac{1}{2L_B} & -\frac{R_{HB}+R_B}{2L_B} \end{bmatrix} \begin{bmatrix} i_L \\ V_C \\ i_B \end{bmatrix} \\
 &+ \begin{bmatrix} \frac{2(1-D_0)R_{HB}}{L} \\ -\frac{1}{(1-D_0)R_{HB}} \\ -\frac{1}{L_B} \end{bmatrix} [i_d] \\
 &+ \begin{bmatrix} \frac{(1-D_0)}{L} \\ 0 \\ 0 \end{bmatrix} [v_{pv}] \\
 &+ \begin{bmatrix} 0 \\ 0 \\ -\frac{1}{L_B} \end{bmatrix} [V_B] \quad (16)
 \end{aligned}$$

Fig. 4 demonstrates the positive bearings of the battery current, i_B , and the network side AC current, i_g .

Fig. 5 demonstrates the square outline for topology. It comprises of three circles: the PV current i_{pvloop} , matrix current i_{gloop} and the battery current i_{Bloop} .

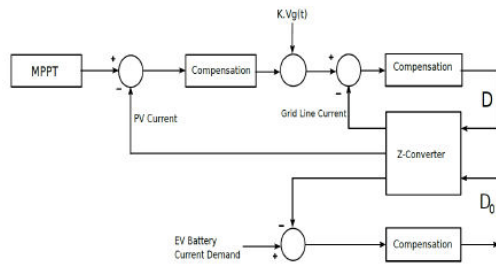


Fig. 5. Square graph of the Control Scheme Proposed Modified Zsource Inverter Charger. In writing, the ZSI capacitor voltage is controlled to produce the reference current for the H-convert inverter yield current [11] or create the shootthrough obligation proportion D_0 [12]. In this article the reference current is produced by controlling the pinnacle input photovoltaic current [13]. On the off chance that a solid voltage V_C is associated crosswise over either or the two capacitors, the shoot through obligation proportion, D_0 , will rely upon V_C . Since the battery current circle don't require quick powerful changes battery circle control is the slowest reaction contrasted with the information current control. For the battery circle control

the exchange capacity is given by:

$$\frac{I_B(s)}{d_0(s)} = \frac{-sC[4R_{HB}i_L - 2R_{HB}i_d] - [2i_L - i_d]}{2L_BCs^2 + sC[R_{HB} + 2R_B] + 0.25} \quad (17)$$

A feed forward is added to the battery control loop,

$$FF_B = \frac{2V_B - v_{PV}}{4V_B - v_{PV}} \quad (18)$$

where V_B is the yield voltage of the HBC and v_{PV} is the followed PV voltage.

The yield AC side current controller ought to have the quickest reaction.

F. Energy Management Scheme for the Proposed Converter

Fig. 6 demonstrates a rearranged square outline of the proposed framework. At the point when an ESS is incorporated into a ZSI, the condition (5) is changed as pursues [14]:

$$v_{PV}i_{PV} = v_b i_b + i_{grms} v_{grms} \quad (19)$$

where i_b and v_b are the battery current and voltage. Fig. 6 demonstrates that the single stage AC lattice control P_{g} balances the power variance of the photovoltaic source P_{pv} thus a steady charge control, P_B , is acquired at the ESS. For EV battery charging utilizing both the single stage AC lattice & photovoltaic power, the heading of the AC framework current i_g changes to negative while drawing power from the matrix.

The inverter side can be worked bidirectionally and the PV & framework gives capacity to the charger, keeping up the power balance.

$$v_{PV}i_{PV} + i_{grms}v_{grms} = v_b i_b \quad (20)$$

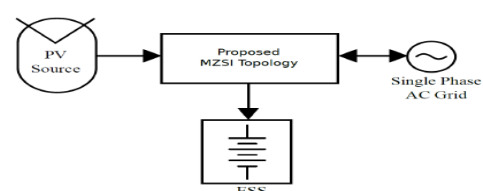


Fig. 6. Simplified Block Diagram of the System

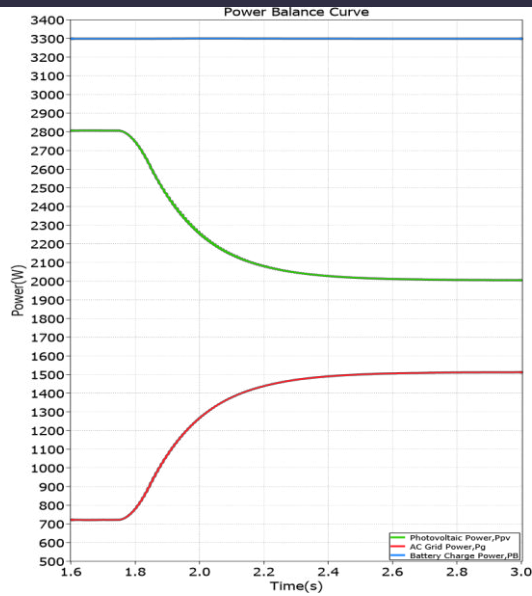


Fig. 7. Simulation Waveform for the power balance between the Photovoltaic input power, the AC Grid side and the battery power.

For whatever length of time that the voltage over the info capacitor C_{in} is kept up to at least the base estimation of the PV voltage, the MZSI can be worked as a lattice associated rectifier/charger without the PV [15]-[16]. Against islanding security methods for the ZSI topology have been tended to in writing already in [17].

IV. SIMULATION AND EXPERIMENTAL RESULTS

A. Simulation study for a MZSI operation

The reproduction concentrates to show the conduct of the proposed topology have been completed utilizing PLECS 4 for a 3.3 kW charger for a string inverter design. Recreation has been completed for the framework appeared in Fig. 2. Fig. 7 appears at reenactment time $t = 1.75$ s, the information PV power lessens from 2.8 kW to 2 kW, the matrix power increments from 710 W to 1500 W to keep up the yield charger capacity to 3.3 kW and the relating lattice current, DC interface voltage, appeared in Fig. 8.

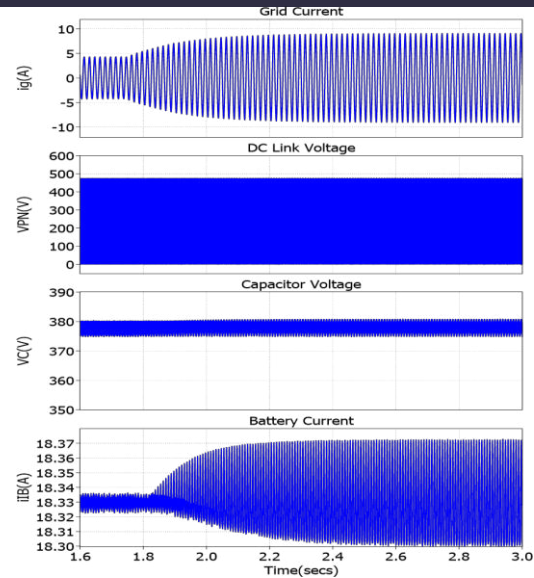


Fig. 8. Reproduction Waveform of the lattice current, I_g , DC connect voltage, V_{PN} , Capacitor Voltage, V_{C1} , and Battery current, i_B for the power balance between the Photovoltaic info control, the AC Grid side and the battery control.

Table I: Modified Z_{si} Based Charger System Simulation Specifications

Parameters	Value
Input Voltage, V_{in}	286 V
Input Current, I_{in}	9.8 A
Inductor Value, $L_1=L_2$	500 μ H
ZSI Switching Frequency, F_{SW}	25 kHz
Grid Voltage (RMS), V_g	240 V
Inverter Output Filter Inductor, L_f	7.5 mH
PV Input Power, P_{PV}	2.8 kW
Input Capacitor, C_{in}	2 mF
HBC Switching Frequency, f	50 kHz
HBC Output Filter, L_B	1 mH
Battery charge power, P_B	3.3 kW

Table II: Component Models Used For Loss Modeling Of The Proposed System

Component	Value
Diode, D	STTH6010W
ZSI MOSFETs [S_A, S_B, S_C and S_D]	APT28M120L
HBC MOSFETs [$S_{AHB}, S_{BHB}, S_{CHB}$ and S_{DHB}]	APT28M120L
HBC Diodes, [$S'_{AHB}, S'_{BHB}, S'_{CHB}$ and S'_{DHB}]	STTH6010W
Capacitor, C_{in}, C_1 and C_2	ECE-T2VP182FA

B. Loss Modeling

The misfortune demonstrating for the proposed framework appeared in Fig. 2 has been done by displaying the real segments in PLECS 4.0. The exchanging parts utilized for the displaying is appeared in the Table II, For the misfortune demonstrating of the uninvolved segments, interior opposition of

the inductors, L_1 , L_2 and L_{fare} $r=100$ m ω and the ESR, RHB for the capacitors C_1 , C_2 and C_{in}

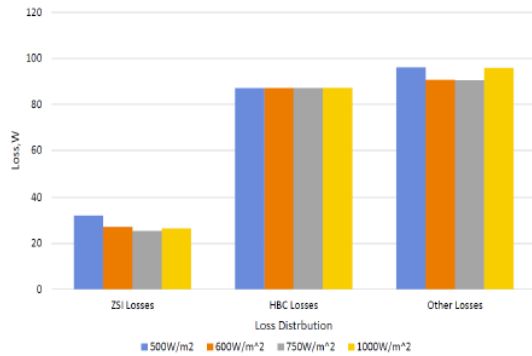


Fig. 9. Misfortune appropriation outline for influence $P_B=3.3$ kW at 25°C , under shifting light

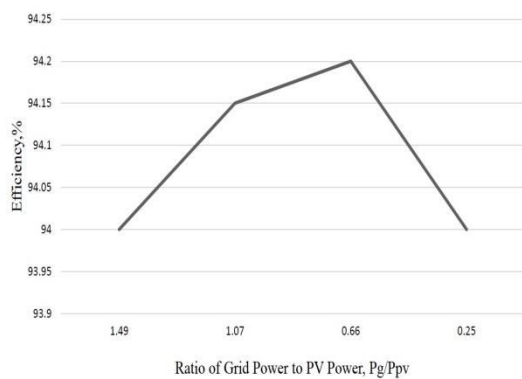


Fig. 10. Efficiency curve for different ratios of AC Grid Power P_g to Photovoltaic Power P_{pv} curve for a fixed charging power $P_B=3.3$ kW at 25°C under varying irradiation are 138 m Ω .

Fig.9 demonstrates the misfortune circulation between the ZSI (conduction and exchanging misfortunes of diode D), the HBC (exchanging misfortunes of the MOSFETs and optional diodes) and different misfortunes in because of the inductor, capacitors, spillage misfortunes in the high recurrence transformer and battery arrangement protections in the framework for shifting lights for a consistent charging influence $P_B=3.3$ kW. Fig.10 demonstrates the effectiveness is around 94% from the proficiency bend for different proportions of AC Grid Power, P_g , to Photovoltaic Power, P_{pv} for a fixed charging power, $P_B=3.3$ kW

at 25°C , for shifting light $500\text{W}/\text{m}^2$ to $1000\text{W}/\text{m}^2$. In spite of the fact that the productivity varieties is little, the effectiveness is the most elevated when the sharing between the photovoltaic power P_{pv} and the framework control P_{gis} equivalent. For a steady recurrence of operation, the HBC MOSFET misfortunes stay consistent for a fixed worth V_B and charging power, P_B . In spite of the fact that as a general rule, this probably won't be the situation. The effectiveness of the converter will change with the adjustment in the battery voltage. Fig.11 demonstrates the dispersion of the misfortunes between the ZSI losses, the HBC MOSFETs and the misfortunes due

Fig. 11. Misfortune circulation for different battery voltages, V_B , for a fixed charging power, $P_B=3.3$ kW, at 45°C

Table III: Modified Z_{si} Based Charger System Prototype Electrical Specifications

Parameters	Value
Input Voltage, V_{in}	38 V
Input Current, I_{in}	3.82 A
Inductor Value, L_1 & L_2	500 μH
Peak DC Link Voltage, V_{PN}	63.33 V
Modulation Index, M	0.75
Shoot Through Duty Ratio, D_{0MAX}	0.2
Switching Frequency, F_{SW}	25 kHz
Grid Voltage, V_g	34 V(RMS)
Inverter Output Filter Inductor, L_f	2.5 mH
HBC switching frequency, f_{HBC}	50 kHz

to the inductor, misfortunes in the high recurrence transformer and battery arrangement protections in the framework for different battery voltages. From Fig.11, at 45°C , the v_{pv} drops to 258V and it tends to be seen that with the expansion in battery voltage the ZSI misfortunes increment yet the HBC misfortunes and the misfortunes in the uninvolved parts diminish.

C. Experimental Verification of the MZSI power balance operation

In this paper as verification of idea, a downsized 175W test arrangement was assembled utilizing MATLAB/Simulink and

dSPACE 1103. The arrangement has the accompanying particulars appeared in table III.

Fig. 12 demonstrates the PWM logic for the HBC. Every one of the split essential work for a large portion of the HBC exchanging period.

Each MOSFET SAHB, SBHB, SCHB and SDHB works solely for one fourth of the whole HBC exchanging period. Condition (23) can be written as far as the present

$$i_{PV} = \frac{1 - D_0}{2(1 - 2D_0)} i_b + \frac{M}{\sqrt{2}(1 - 2D_0)} i_g \quad (21)$$

where M is the modulation index and D₀ is the shootthroughduty ratio. For D₀=0.2,

$$i_{PV} = \frac{2}{3} i_b + \frac{\sqrt{3}}{2} i_g \quad (22)$$

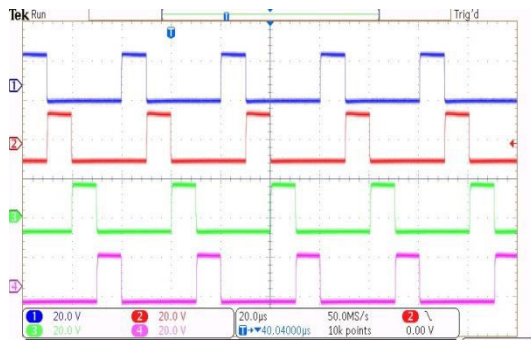


Fig. 12. PWM logic for the isolated HBC

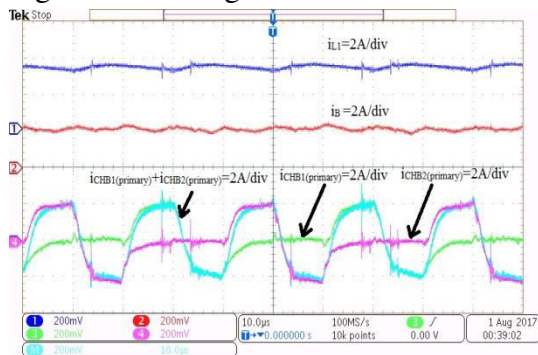


Fig. 13. Experimental setup waveforms for the Inductor current (top), charger output current (middle) and the primary currents of the split charger (bottom) From equation (22), at D₀=0.2, for an input current i_{PV}=3.82 A and fixed HBC output current i_b=2 A, the ZSI AC output current i_g is calculated to be 2.87 A. From condition (22), at D₀=0.2, for an info current i_{PV} =3.82A and fixed HBC yield

current i_b=2 A, the ZSI AC output current i_g is determined to be 2.87 A.

Fig.13 demonstrates the inductor current i_{L1}, the battery current i_B and the split essential current i_{CHB1} and i_{CHB2} and the total essential current. Every one of the essential work alternately. The all out essential current is a high recurrence alternating current of f_{HBC}=50 kHz. From Fig. 13 and Fig. 14, the charger output current is maintained at 2 A utilizing a Chroma Programmable AC/DC Electronics Load (Model 6304). The PV input current is maintained at 3.82 A utilizing a Magna-control LXITM sun powered emulator. The yield framework current is seen to be 2.66 A. Fig. 15 shows the trial arrangement for the confirmation of idea. The lower estimations of the yield current is an aftereffect of the losses in the circuit. The useful PI esteems for the AC side current control was K_P =0.03 and the battery circle was K_{PB}=0.0003 and K_{IB}=0.09 and the information PV current circle were K_{Pin}=0.005 and K_{Iin}=2.

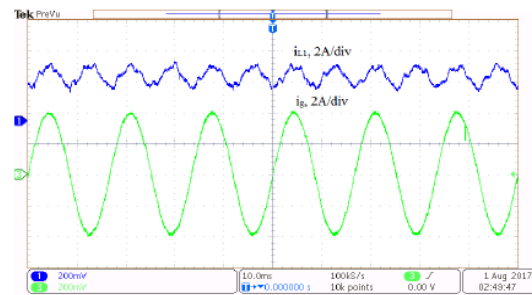


Fig. 14. Test waveform input current (blue) and yield current (green) between the charger and the AC yield of the MZSI

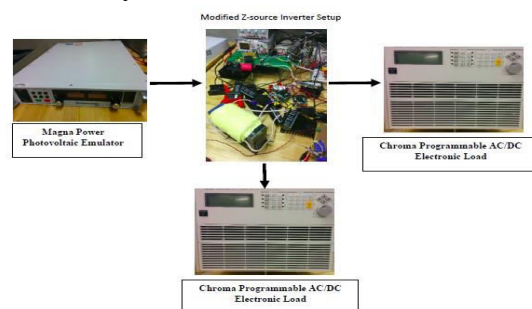


Fig. 15. Experimental setup

Table IV: Isolated HalfBridge Dc-Dc SystemElectricalSpecifications

Parameters	Value
Input Voltage, V_C	50.667 V
Output Voltage, V_B	25.335 V
Switching Frequency, $F_{sw}(HB)$	50 kHz
Filter inductor, L_B ,	330 μ H

V. CONCLUSION

A changed ZSI topology has been proposed in this paper is an alluring answer for photovoltaic matrix associated charging frameworks. It comprise of a solitary stage photovoltaic lattice (PV-Grid) association and a coordinated charger for PV-Grid associated charging or vitality stockpiling. This topology can be connected to brought together setup for charging in semi-business areas, for example, a parking area of a shopping center. For private applications, this thought can be reached out to string inverters with the charger side of the string inverter designs associated in arrangement or parallel for current sharing.

REFERENCES

1. D. Aggeler, F. Canales, H. Zelaya, D. L. Parr a, A. Coccia, N. Butcher, and O. Apeldoorn, "Ultra-fast dc-charge infrastructures for ev-mobility and future smart grids," in Proc. of IEEE PES Innovative Smart Grid Technologies Conference Europe, pp. 1–8, Oct. 2010.
2. G. Carli and S. S. Williamson, "Technical considerations on power conversion for electric and plug-in hybrid electric vehicle battery charging in photovoltaic installations," IEEE Trans. on Ind. Electron., vol. 28, no. 12, pp. 5784–5792, 2013.
3. J. G. Ingersoll and C. A. Perkins, "The 2.1 kw photovoltaic electric vehicle charging station in the city of santamonica, california," in Proc. of the Twenty Fifth IEEE Photovoltaic

Specialists Conference, pp. 1509–1512, May. 1996.

4. S. B. Kjaer, J. K. Pedersen, and F. Blaabjerg, "A review of single-phase grid-connected inverters for photovoltaic modules," IEEE Trans. on Ind. Appl., vol. 41, no. 5, pp. 1292–1306, Sep. 2005.
5. N. A. Ninad, L. A. C. Lopes, and I. S. Member, "Operation of Single-phase Grid-Connected Inverters with Large DC Bus Voltage Ripple," Proc. of the IEEE Canada Electrical Power Conference, 2007.
6. S. Bai, D. Yu, and S. Lukic, "Optimum design of an ev/phev charging station with dc bus and storage system," in Proc. of IEEE ECCE, pp. 1178–1184, Sep. 2010.
7. F. Z. Peng, "Z-Source Inverter," in IEEE Trans. on Ind. Appl., vol. 39, no. 2, pp. 504–510, 2003.
8. Y. Huang, M. Shen, F. Z. Peng, and J. Wang, "Z-source inverter for residential photovoltaic systems," IEEE Trans. on Power Electron., vol. 21, no. 6, pp. 1776–1782, Nov. 2006.
9. S. A. Singh, N. A. Azeez, and S. S. Williamson, "Capacitance reduction in a single phase quasi z-source inverter using a hysteresis current controlled active power filter," in Proc. of IEEE 25th Int. Symp. on Ind. Electron., pp. 805–810, Jun. 2016.
10. S. A. Singh, G. Carli, N. A. Azeez, and S. S. Williamson, "A modified z-source converter based single phase pv/grid inter-connected dc charging converter for future transportation electrification," in Proc. of IEEE ECCE, pp. 1–6, Sep. 2016.
11. Y. Li, S. Jiang, J. G. Cintron-Rivera, and F. Z. Peng, "Modeling and control of quasi-z-source inverter for distributed generation applications," IEEE Trans. on



Ind.Electron., vol.60, no.4,pp.1532–1541, Apr.2013.

12. T. Chandrashekhar and M. Veerachary, “Control of single-phase z-source inverter for a grid connected system,” in Proc.ofInt.Conf.onPowerSyst.,pp.1–6,Dec. 2009.

13. B.Ge,Y.Liu,H.Abu-Rub,R.S.Balog, F.Z.Peng,S.McConnell,andX.Li, “Current ripple damping control to minimize impedance network for single-phase quasi-z source inverter system,” IEEETransonInd.Info.,vol.12,no.3,pp.1043–1054, Jun. 2016.